JOURNAL OF ELECTROMAGNETIC ENGINEERING AND SCIENCE, VOL. 22, NO. 6, 631~637, NOV. 2022

https://doi.org/10.26866/jees.2022.6.r.132
ISSN 2671-7263 (Online) · ISSN 2671-7255 (Print)

Design of a Wideband Printed Patch Dipole Antenna with a Balanced On-Board Feeding Network

Jeongmin Cho[1] · Tae Heung Lim[2,*] · Youngwan Kim[3] · Hosung Choo[1]

Abstract

This paper proposes a wideband printed patch dipole antenna with a simple on-board feeding network. The proposed antenna is composed of two dipole radiators, a transmission line, and an on-board feeding network with a chip balun. The dipole radiators are printed on a substrate, and the edges of the radiators are truncated to create a hexagonal shape with wide impedance-matching characteristics. The chip balun is embedded in an RO4003C printed circuit board (PCB) to excite differential feeding to each radiator with a 180° phase difference. The proposed antenna is optimized using a CST Studio full electromagnetic software tool, and it is fabricated and measured in an anechoic chamber. The measured fractional bandwidth for the reflection coefficient below –10 dB is 79.5%, and the proposed antenna has a measured gain of 7.1 dBi at 3.5 GHz.

Key Words: Dipole Patch Antenna, Equivalent Circuit Analysis, On-Board Chip Balun Antenna, S-Band Antenna, Wideband Antenna.

I. Introduction

Dipole antennas have been widely used for various applications, including wireless communication systems, radar systems, and localization systems [1–6]. Recent developments in system design technologies have led such systems to become small in platform size and to include multiple functions, such that the systems have required a wide operating frequency band, high integration, size miniaturization, and high radiation performance. In particular, the wide impedance-matching characteristics of dipole antennas are essential for operating multifunctional systems, and their directive radiation patterns are important for stably maintaining point-to-point communication links. To obtain wideband characteristics, 3D dipole antennas have been investigated using a biconical structure [7, 8], an additional parasitic element [9], and an indirect feeding structure [10]. However, these studies have difficulties with high integration into systems due to the bulky structure size and nondirective radiation patterns. To overcome these problems, printed patch dipole antennas for directive patterns have been introduced by employing various shapes, such as an ellipse, a bow tie, and a polygon [11–13]. Although such antennas can achieve wideband characteristics with stable boresight gains, it is essential that additional bulky baluns are elaborately designed for differential feeding to excite each radiator with a 180° phase difference [14]. To account for the additional baluns, research on using a small chip balun has been conducted to achieve size reduction of the differential feeding structure [15, 16]. However, their matching bandwidth is still narrow, lower than 10%, and an in-depth study is needed to analyze patch dipole antennas with integrated circuit baluns.

Manuscript received March 2, 2022 ; Revised April 26, 2022 ; Accepted June 1, 2022. (ID No. 20220302-022J)
[1]Department of Electronic and Electrical Engineering, Hongik University, Seoul, Korea.
[2]Department of Electrical Engineering, Ulsan National Institute of Science and Technology (UNIST), Ulsan, Korea.
[3]Radar Research Institute, LIG Nex1, Yongin, Korea.
[*]Corresponding Author: Tae Heung Lim (e-mail: limth0105@unist.ac.kr)

In this paper, we propose a wideband printed patch dipole antenna with a simple on-board feeding network. The proposed antenna is composed of two dipole radiators, a transmission line, and an on-board feeding network with a chip balun. The dipole radiators are printed on a substrate, and the edges of the radiators in the center of the substrate are truncated to create a hexagonal shape for direct connection with the transmission line and for wide impedance-matching characteristics. In addition, the transmission line is designed to operate as a quarter-wave transformer for impedance matching between the dipole radiators and the chip balun. The chip balun is embedded in an RO4003C printed circuit board (PCB) to excite differential feeding to each radiator with a 180° phase difference. This chip balun, which can reduce the size of the feeding network structure, is fed by a microstrip line and an SMA connector. The proposed antenna, including the chip balun circuit, is optimized using the CST Microwave Studio software tool [17]. To verify its feasibility, the proposed antenna is fabricated, and its antenna properties, such as reflection coefficients, radiation patterns, and gains, are measured in a full anechoic chamber. For antenna analysis, an equivalent circuit of the proposed antenna is modeled to analyze its impedance characteristics, and parametric studies are conducted to achieve wideband characteristics.

II. Proposed Antenna Design and Measurement

Fig. 1 shows the geometry of the proposed antenna composed of two dipole patch radiators, a parallel plate transmission line, and a feeding network with a chip balun. The patch dipole antenna is printed on a TLY-5 substrate ($\varepsilon_r = 2.2$, $\tan\delta = 0.0009$) having dimensions $w_3 \times l_3 \times t_1$ (width × length × thickness). The dipole patches have a length l_1 that can determine the resonant frequency, and its width w_1 can enhance the impedance-matching characteristics at the resonant frequency. To achieve wideband characteristics, the radiator edges in the center of the substrate are truncated by width d_1 and length d_2. Note that a half-wavelength dipole antenna length generally has a single operating frequency with a narrow bandwidth [18], while a patch dipole can achieve a wideband characteristic by changing the width and length of the radiator, allowing a different current path for each operating frequency [19]. Thus, the geometry of the radiators becomes hexagonal, which can directly connect to the transmission line. In addition, the wide impedance-matching characteristics can be further improved by adjusting the slope of the truncated part for the radiators. The parallel plate transmission line printed on the TLY-5 substrate has a width w_2 and a length l_2. This transmission line is perpendicularly connected to the truncated part of the dipole radiators having a gap t_2. In particular, l_2 can be operated as a quarter-wave transformer to match the impedance between the dipole radiators and the chip balun. The feeding network is designed using an RO4003C ($\varepsilon_r = 3.35$, $\tan\delta = 0.0027$) PCB with a chip balun and differential microstrip lines to substitute for the bulky and complicated microstrip balun. The differential feeding lines having a length l_4 and a width w_4 are designed to have a line impedance of 100 Ω, and they are connected to each radiator by two via pins for a 180° phase difference excitation. An SMA connector is used to excite a signal for the chip balun through the microstrip line with width w_5 and length l_5.

The proposed antenna is optimized using a CST Studio full electromagnetic (EM) software tool including 3D EM modeling and a circuit schematic, which are sequentially simulated to obtain the impedance characteristics of the antenna and the PCB feeding network. The antenna radiators and the parallel transmission lines of the proposed antenna are simulated by 3D EM modeling of the structures. The PCB feeding network is designed based on a schematic layout, including the chip balun *S*-parameter, the microstrip feeding line, and the microstrip differential lines. Through the sequential simulations, the optimized design parameters and values are listed in Table 1.

Fig. 2 presents photographs of the fabricated antenna consisting of the dipole radiators, the transmission line, and the chip

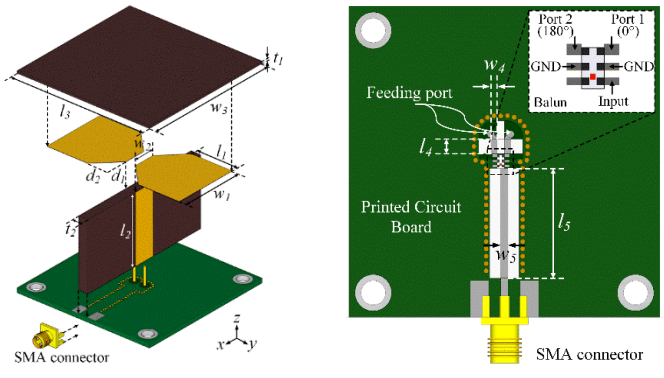

Fig. 1. Geometry of the proposed antenna: (a) isometric view and (b) bottom view.

Table 1. Geometric parameters of the proposed antenna (unit: mm)

Parameter	Value	Parameter	Value
w_1	40	l_3	45.2
w_2	3	l_4	3.5
w_3	51	l_5	13.4
w_4	1.1	t_1	0.8
w_5	1.1	t_2	3.2
l_1	14	d_1	18.5
l_2	29.7	d_2	7

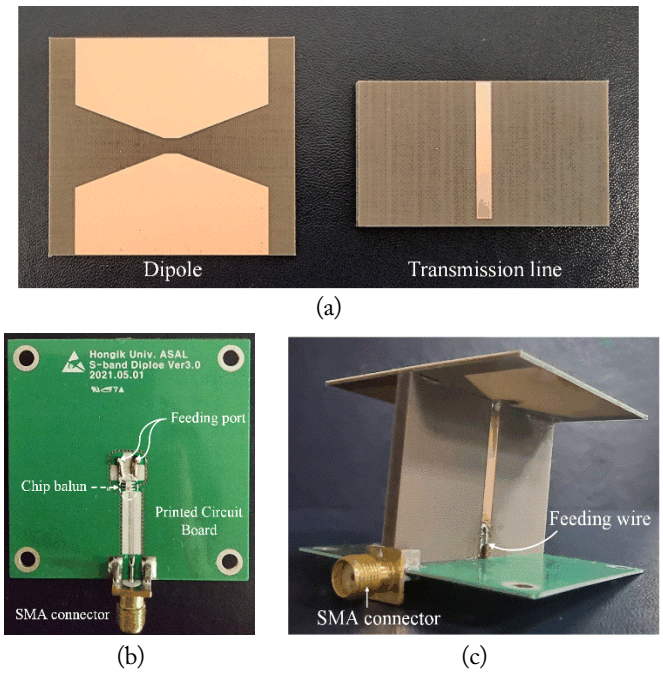

Fig. 2. Configuration of the fabricated antenna: (a) dipole radiators and parallel plate transmission line, (b) PCB feeding network, (c) assembled antenna.

balun embedded in the PCB feeding network. It is essential to use a chip balun operating in a wide frequency band that incorporates the dipole radiator to achieve wideband characteristics. Thus, we employ the Johanson Technology chip balun (balanced impedance of 100 Ω from 2.8 to 6 GHz) [20] to excite differential feeding with a 180° phase difference to each dipole radiator. To verify its feasibility, the fabricated antenna is measured in a full anechoic chamber to observe antenna performances, such as reflection coefficients, gains, and radiation patterns.

Fig. 3 represents the reflection coefficients of the proposed antenna; solid and dashed lines indicate the measured and simulated results, respectively. The measured and simulated reflection coefficients are below –10.5 dB and –11 dB, respectively, in the frequency range from 2.7 to 5.8 GHz. The measured and simulated fractional bandwidths at the center frequency of 4 GHz are 79.5% and 83.4%, respectively. Fig. 4 shows the boresight gains of the proposed antenna according to frequency. The solid line and the "×" markers indicate the simulations and measurements, respectively. Both simulated and measured gains are over 3 dBi in the frequency range from 2.75 to 4.5 GHz. Fig. 5 illustrates the measured and simulated 2D radiation patterns of the proposed antenna in the *zx*- and *zy*-planes at 3.5, 4.5, and 5.5 GHz. The measured cross-polarization levels at the boresight direction are lower than –17.5 dBi and –13.2 dBi in the *zx*- and *zy*-planes, respectively, at 3.5 GHz. The measured results agree well with the simulations. The measured half-power beamwidths (HPBWs) are 107° and 86° in the *zx*- and *zy*-planes at 3.5 GHz, and those at 4.5 GHz are 154° and 94°, respectively. Fig. 6 presents the total efficiency and the radiation efficiency according to frequency. The total efficiency of the proposed antenna considering the mismatch efficiency with frequency is simulated. The total efficiency is over 82% in the operating frequency range from 2.75 to 5.8 GHz, and it is 90.8% at 5.5 GHz. The radiation efficiency value is obtained as more than 98.3% across the whole operating frequency range.

The results demonstrate that the proposed antenna can achieve wideband impedance characteristics and maintain stable gain performance using an on-board balanced chip balun for a simple feeding network. The antenna performances including fractional bandwidth, gain at the center frequency, integrated balun type, and antenna size are listed in Table 2 for comparison with previous studies. The proposed antenna can reduce the antenna size by less than 63% compared with antennas that use Guanella and microstrip line baluns, which have a length and width greater than one wavelength. In addition, the dipole in our study can enhance the impedance-matching bandwidth by more than 79% compared with previous studies that integrated chip baluns.

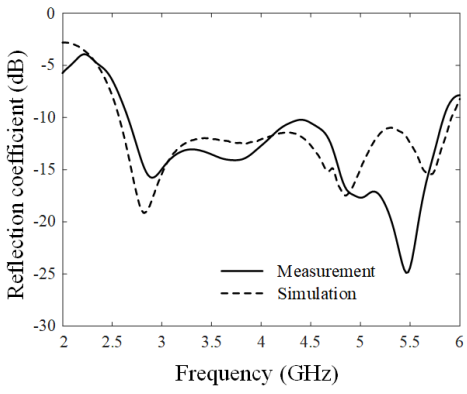

Fig. 3. Simulated and measured reflection coefficients of the proposed antenna.

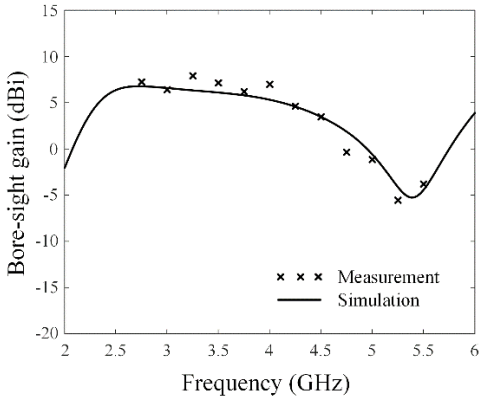

Fig. 4. Simulated and measured bore-sight gains of the proposed antenna.

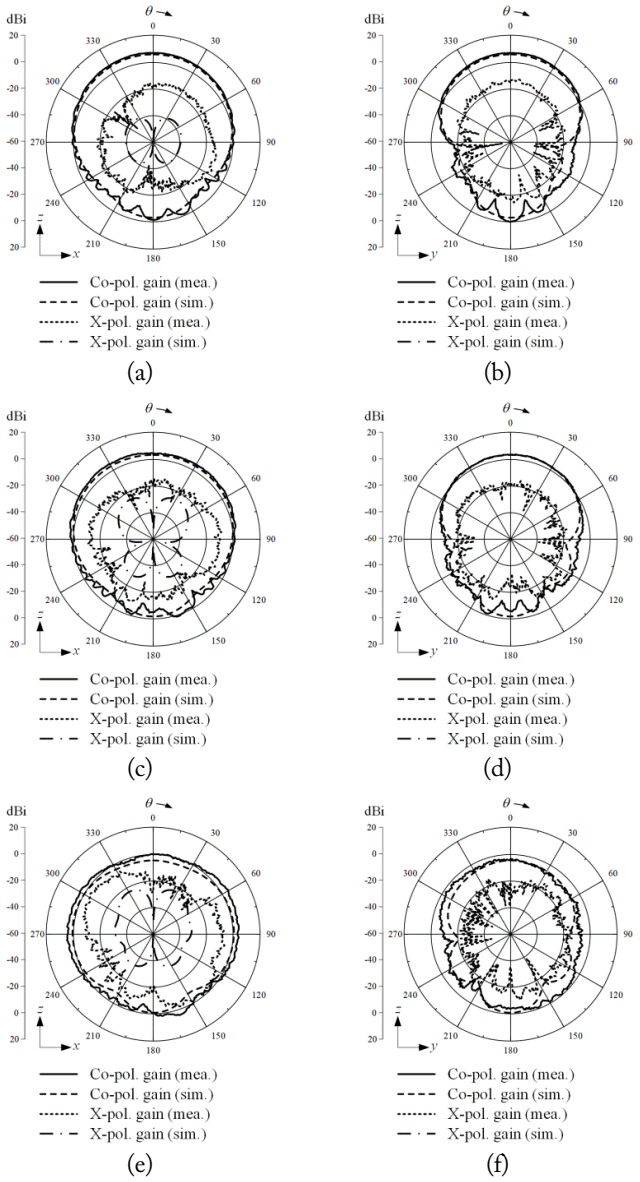

Fig. 5. Simulated and measured 2D radiation patterns of the proposed antenna: (a) *zx*-plane at 3.5 GHz, (b) *zy*-plane at 3.5 GHz, (c) *zx*-plane at 4.5 GHz, (d) *zy*-plane at 4.5 GHz, (e) *zx*-plane at 5.5 GHz, (f) *zy*-plane at 5.5 GHz.

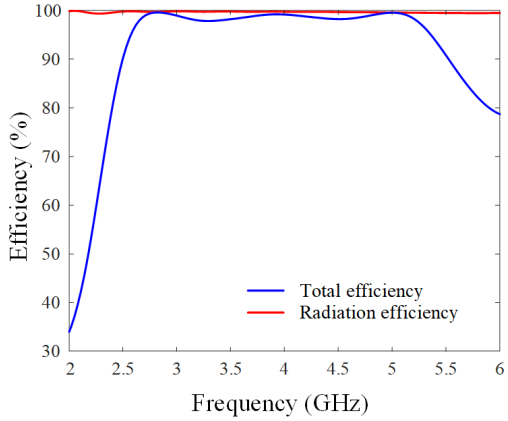

Fig. 6. Total efficiency and radiation efficiency of the proposed antenna.

Table 2. Comparison of antenna characteristics

Study	Band-width (%)	Gain (dBi)	Balun type	Antenna size
Wagner and Pham [11]	171	2.5	Guanella balun	1.2λ × 1.2λ × 0.003λ
Toh et al. [14]	43	8	Microstrip line	1λ × 1λ × 0.13λ
Singh et al. [15]	3.9	2.8	Chip balun	0.48λ × 0.24λ × 0.01λ
Suh et al. [16]	4	-	Chip balun	0.42λ × 0.05λ × 0.01λ
Proposed antenna	83	4.6	Chip balun	0.72λ × 0.64λ × 0.42λ

III. ANALYSIS

To analyze the proposed antenna, an equivalent circuit is modeled, taking into account important antenna parts: the patch radiator, the transmission line, the chip balun, and the feeding port. Fig. 7(a) shows an equivalent circuit model of the proposed antenna including the transmission line, the chip balun, and the antenna resonant circuits to observe the input impedance characteristics. In the circuit model, the SMA port of 50 Ω is modeled as an inductance L_f to excite the 1:2 chip balun with a balanced impedance of 100 Ω. Through the chip balun, the parallel transmission line of the proposed antenna is connected to the parallel RLC element with R_1, L_1, and C_1 representing the resonance of the dipole radiator. In particular, the parallel

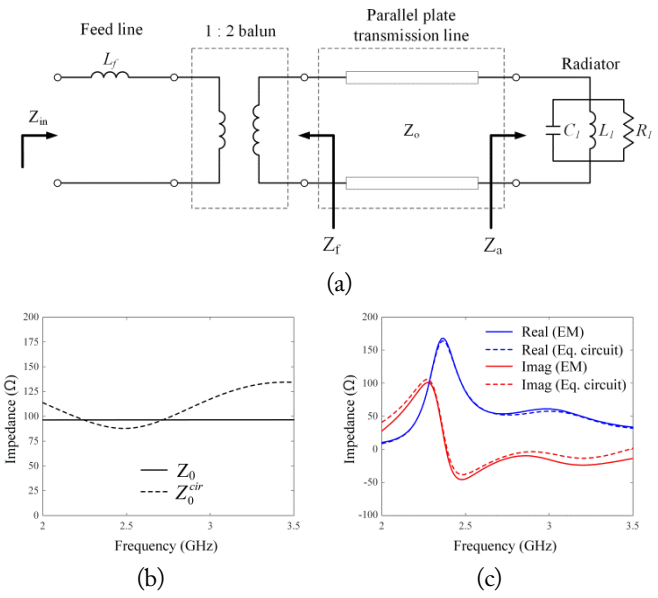

Fig. 7. An equivalent circuit of the proposed antenna with a chip balun: (a) equivalent circuit model, (b) characteristic impedance responses of the parallel plate transmission line, (c) input impedance responses according to the frequency.

plate transmission line is operated as a quarter-wave transformer, and its characteristic impedance can be obtained using an equation as follows [21]:

$$Z_0^{cir} = \sqrt{Z_f Z_a}, \quad (1)$$

where Z_0^{cir} is the characteristic impedance of the parallel plate transmission line from the equivalent circuit model, Z_f is the input impedance of the feeding network, and Z_a is the dipole patch radiator impedance based on parallel RLC elements. Z_0 is the characteristic impedance of the parallel plate transmission line obtained based on a full EM simulation. Fig. 7(b) shows the characteristic impedance responses of the parallel plate transmission line according to the frequency. The simulated and circuit-based characteristic impedance results are 96.45 Ω and 96.41 Ω, respectively, at 2.72 GHz ($l_2 \approx \lambda/4$). The results confirm that the parallel transmission line of the proposed antenna works as a quarter-wave transformer for wideband characteristics. Fig. 7(c) illustrates the input impedance responses of the simulation and the equivalent circuit model according to the frequency, where blue and red lines indicate resistance and reactance values. The results of the equivalent circuit are in good agreement with the simulated results. This shows that the equivalent circuit is well modeled and represented for each part of the proposed antenna. The detailed values of the lumped elements are listed in Table 3.

In addition, parametric studies of w_2 and l_2 are conducted to observe the sensitivity of the reflection coefficients, as shown in Fig. 8. Parameter w_2 can adjust the reflection coefficient levels at the high-end frequency band, and l_2 can affect the operating bandwidth due to the change in the capacitive couplings between the dipole radiator and ground. The optimum w_2 of 3 mm and l_2 of 29.7 mm are then obtained considering the stable reflection coefficient below –10 dB in the operating frequency band.

To further analyze the proposed antenna, parametric studies are conducted considering essential design parameters such as the radiator width (w_1), length (l_1), and truncated part (d_2). In this analysis, we focus on the observation of the fractional bandwidth, and the maximum reflection coefficient. The maximum reflection coefficient is defined as Γ_{max} to observe the stability of the wideband operation for the proposed antenna in the operating frequency band from 2.75 to 5 GHz. Fig. 9(a)–9(c)

Table 3. Parameters of the lumped elements

Parameter	Value
R_1	167 Ω
L_1	3.53 nH
C_1	6.45 pF
L_f	0.015 nH

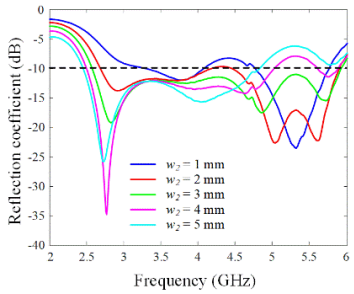

(a)

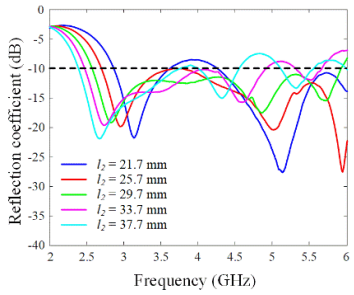

(b)

Fig. 8. Parametric study results according to the transmission line width and length: (a) w_2, (b) l_2.

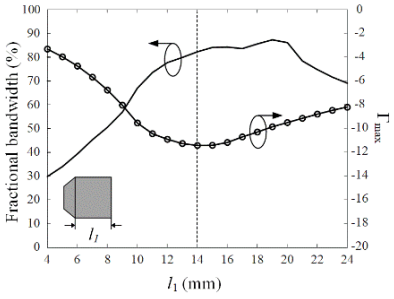

(a)

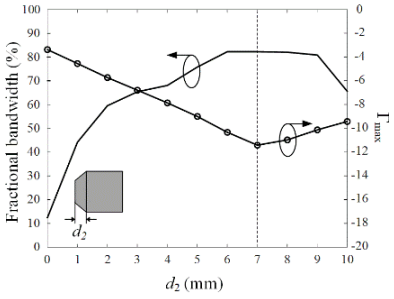

(b)

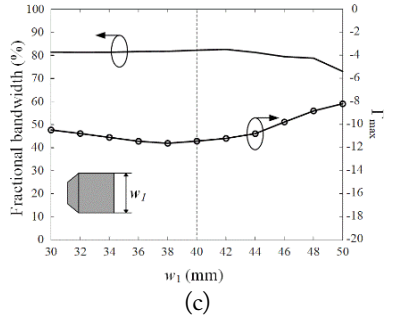

(c)

Fig. 9. Simulated parametric study results: Fractional bandwidth and Γ_{max} according to (a) l_1, (b) d_1, and (c) w_1.

show the simulated parametric study results of the fractional bandwidth, and the maximum reflection coefficient. Results are obtained while varying the parameters in the ranges 4 mm ≤ l_1 ≤ 24 mm, 0 mm ≤ d_2 ≤ 10 mm, and 30 mm ≤ w_1 ≤ 50 mm. Parametric studies indicate that the proposed antenna can achieve an over 80% fractional bandwidth with a Γ_{max} of below –11.4 dB when using optimized parameters (dashed lines).

IV. Conclusion

In this paper, we proposed a wideband printed patch dipole antenna with a simple on-board feeding network. The proposed dipole antenna was printed on a substrate and was directly connected to the transmission line with the on-board balanced chip balun. The proposed antenna had measured and simulated fractional bandwidths of 79.5% and 83.4%, respectively. The simulated and measured gains were over 3 dBi in the frequency range of 2.75 to 4.5 GHz. The measured HPBWs were 107° and 86° in the *zx*- and *zy*-planes, respectively, at 3.5 GHz, and those at 4.5 GHz were 154° and 94°, respectively. To analyze the proposed antenna, an equivalent circuit was modeled, taking into account important antenna parts. The equivalent circuit results confirmed that the parallel transmission line of the proposed antenna worked as a quarter-wave transformer to achieve wideband characteristics. In addition, through parametric studies, the proposed antenna achieved over 80% stable fractional bandwidth with a Γ_{max} of below −11.4 dB. For future work, additional or different designs will further be considered, such as a tapered transmission line and a cavity-backed ground to overcome the pattern distortion in the high-end frequency band.

This research has been supported by the Challenging Future Defense Technology Research and Development Program (No. 9127786) of Agency for Defense Development in 2019.

References

[1] Y. Feng, F. S. Zhang, G. J. Xie, Y. Guan, and J. Tian, "A broadband and wide-beamwidth dual-polarized orthogonal dipole antenna for 4G/5G communication," *IEEE Antennas and Wireless Propagation Letters*, vol. 20, no. 7, pp. 1165-1169, 2021.

[2] J. Zeng and K. M. Luk, "Single-layered broadband magnetoelectric dipole antenna for new 5G application," *IEEE Antennas and Wireless Propagation Letters*, vol. 18, no. 5, pp. 911-915, 2019.

[3] S. V. Pushpakaran, N. M. SeidMuhammed, R. K. Raj, A. Pradeep, P. Mohanan, and K. Vasudevan, "A compact stacked dipole antenna with directional radiation coverage for wireless communications," *IEEE Antennas and Wireless Propagation Letters*, vol. 12, pp. 841-844, 2013.

[4] M. Mirmozafari, S. Saeedi, G. Zhang, and Y. Rahmat-Samii, "A crossed dipole phased array antenna architecture with enhanced polarization and isolation characteristics," *IEEE Transactions on Antennas and Propagation*, vol. 68, no. 6, pp. 4469-4478, 2020.

[5] J. D. Hawkins, L. B. Lok, P. V. Brennan, and K. W. Nicholls, "HF wire-mesh dipole antennas for broadband ice-penetrating radar," *IEEE Antennas and Wireless Propagation Letters*, vol. 19, no. 12, pp. 2172-2176, 2020.

[6] D. Jang, J. Hur, H. Shim, J. Park, C. Cho, and H. Choo, "Array antenna design for passive coherent location systems with non-uniform array configurations," *Journal of Electromagnetic Engineering and Science*, vol. 20, no. 3, pp. 176-182, 2020.

[7] C. SaiRam, D. Vakula, and M. Chakravarthy, "Design of broadband compact canonical triple-sleeve antenna operating in UHF band," *Journal of Electromagnetic Engineering and Science*, vol. 21, no. 4, pp. 291-298, 2021.

[8] S. He, L. Chang, and Z. Z. Chen, "Design of a compact biconical antenna loaded with magnetic dipoles," *IEEE Antennas and Wireless Propagation Letters*, vol. 16, pp. 840-843, 2016.

[9] L. Chang, L. L. Chen, J. Q. Zhang, and Z. Z. Chen, "A compact wideband dipole antenna with wide beamwidth," *IEEE Antennas and Wireless Propagation Letters*, vol. 20, no. 9, pp. 1701-1705, 2021.

[10] S. Wang, J. Park, H. Shim, and H. Choo, "Design of a wideband coupled feed dipole antenna for PCL array systems," *Journal of Electrical Engineering & Technology*, vol. 15, no. 5, pp. 2251-2258, 2020.

[11] S. Wagner and A. V. Pham, "The ultrawideband elliptical resistively loaded vee dipole," *IEEE Transactions on Antennas and Propagation*, vol. 68, no. 4, pp. 2523-2530, 2020.

[12] G. Feng, L. Chen, X. Wang, X. Xue, and X. Shi, "Broadband circularly polarized crossed bowtie dipole antenna loaded with parasitic elements," *IEEE Antennas and Wireless Propagation Letters*, vol. 17, no. 1, pp. 114-117, 2018.

[13] Y. He, W. He, and H. Wong, "A wideband circularly polarized cross-dipole antenna," *IEEE Antennas and Wireless Propagation Letters*, vol. 13, pp. 67-70, 2014.

[14] W. K. Toh, X. Qing, and Z. N. Chen, "A planar UWB patch-dipole antenna," *IEEE Transactions on Antennas and Propagation*, vol. 59, no. 9, pp. 3441-3443, 2011.

[15] J. Singh, R. Stephan, and M. A. Hein, "Low-profile wideband differentially fed di-patch antenna closely above metallic ground," *IEEE Antennas and Wireless Propagation Letters*, vol. 18, no. 5, pp. 976-980, 2019.
[16] S. Y. Suh, V. K. Nair, A. Konanur, U. Karacaoglu, and K. H. Lee, "Wireless performance improvement using an embedded balanced dipole antenna in laptop computer considering platform noise impact," in *Proceedings of 2008 IEEE Antennas and Propagation Society International Symposium*, San Diego, CA, 2008, pp. 1-4.
[17] CST Studio Suite: electromagnetic field simulation software [Online]. Available: http://www.cst.com.
[18] C. A. Balanis, *Antenna Theory Analysis and Design*, 3rd ed. New York, NY: Wiley, 2005, pp. 182-184.
[19] Y. M. Guo, Y. Z. Yin, J. L. Gou, J. P. Ma, and H. L. Zheng, "Wideband patch dipole antenna," in *Proceedings of 2005 IEEE Antennas and Propagation Society International Symposium*, Washington, DC, 2005, pp. 561-564.
[20] Johanson Technology, "4400BL15A0100 datasheet," 2020 [Online]. Available: https://www.johansontechnology.com/datasheets/4400BL15A0100/4400BL15A0100.pdf.
[21] D. M. Pozar, *Microwave Engineering*, 4th ed. New York, NY: Wiley, 2012, pp. 246-249.

Jeongmin Cho

received his B.S. degree in electronic and electrical engineering from Hongik University, Seoul, South Korea, in 2021. He is currently working toward his M.S. in electronic and electrical engineering from Hongik University, Seoul, South Korea. His research interests include shared aperture radar, wave propagation for radar applications, and X-band radar antennas.

Tae Heung Lim

received his B.S., M.S., and Ph. D degrees in electronic and electrical engineering from Hongik University, Seoul, South Korea, in 2016, 2018, and 2022, respectively. He is currently working as a postdoctoral researcher in electrical engineering at Ulsan National Institute of Science and Technology (UNIST), South Korea. His research interests include global positioning system antennas, time-modulated arrays, antenna arrays, position optimization of array elements for adaptive beamforming, and wave propagations for radar applications.

Youngwan Kim

received his B.S. and M.S. degrees in radio engineering from Kwangwoon University, Seoul, South Korea, in 2005 and 2007, respectively. He has been a chief research engineer with LIG Nex1, where he has been involved in the development of antennas for radar systems. His research interests include array antennas and metamaterials.

Hosung Choo

received his B.S. degree in radio science and engineering from Hanyang University in Seoul, South Korea, in 1998, and his M.S. and Ph.D. degrees in electrical and computer engineering from the University of Texas at Austin, in 2000 and 2003, respectively. In September 2003, he joined the School of Electronic and Electrical Engineering, Hongik University, Seoul, South Korea, where he is currently a full-time professor. His principal areas of research are the use of optimization algorithms for developing antennas and microwave absorbers. His research includes the design of small antennas for wireless communications, reader and tag antennas for RFID, and on-glass and conformal antennas for vehicles and aircraft.